Journal of Materials Chemistry A

Accepted Manuscript

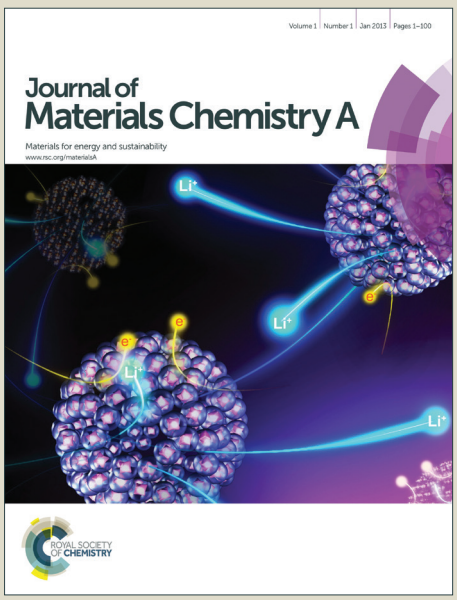

ROYAL SOCIETY OF CHEMISTRY

www.rsc.org/materialsA

Graphic Abstract

A click-based porous organic framework (POF) containing terdentate 2,6-bis(1,2,3-triazol-4-yl)pyridyl units has been prepared. The terdentate unit serves as both linakge of the POF and stabilizer of palladium nanopaticles, the excellent catalytic activity, high stability and good reusability were shown in palladium-catalyzed hydrogenation of olefins.

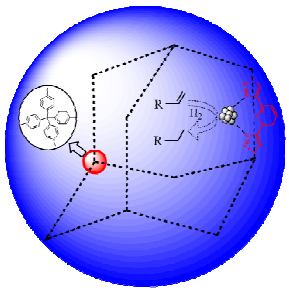

Highlight text: A click-based porous organic framework containing pyridyl-centered terdentate chelating units serves as an efficent support of plladium nanoparticles in hydrogenation.

Cite this: DOI: 10.1039/c0xx00000x

www.rsc.org/xxxxxx

ARTICLE TYPE

Click-based Porous Organic Framework Containing Chelating Terdentate Units and Application in Hydrogenation of Olefins

Hong Zhong,[a,b] Yaqiong Gong,[a] Fengshen Zhang,[a,b] Liuyi Li,[a,b] and Ruihu Wang [a,b]*

Received (in XXX, XXX) Xth XXXXXXXXX 20XX, Accepted Xth XXXXXXXXX 20XX

DOI: 10.1039/b000000x

Click reaction of 2,6-diethynylpyridine and tetrakis(4-azidophenyl)methane gave rise to a porous organic framework containing chelating terdentate 2,6-bis(1,2,3-triazol-4-yl)pyridyl units (BTP-POF). BTP can serve as a promising linkage of organic framework and as an effective stabilizer of palladium nanoparticles (NPs) owing to its structural preference and strong chelating ability with palladium. The well-dispersed palladium NPs in interior pores and external surface of BTP-POF were readily obtained, The NPs in interior pores possess small size and narrow size distribution, they show excellent catalytic activity, high stability and good reusability in palladium-catalyzed hydrogenation of olefins at 25 °C. The mean diameter of palladium NPs was increased from 1.8 to 2.5 nm after recycling for seven runs, but no obvious loss of catalytic activity and agglomeration of palladium NPs were observed. Mercury drop test, filtration experiment and ICP analysis suggest that Pd/BTP-POF is a heterogeneous catalytic system in hydrogenation of olefins.

1. Introduction

The search of new supports for highly active and recyclable heterogeneous catalysts is one of the priorities in modern organic synthesis, especially for chemical and pharmaceutical industries.[1] Porous organic frameworks (POFs) are one of promising supports because of their large surface area, low skeleton density, flexible synthetic strategy, ready functionality and high stability.[2] The intense and continuous efforts have led to rapid development of various POFs with interesting structures and properties, but there is a pressing requirement for design and synthesis of POFs containing specific functional groups to improve their application in heterogeneous catalysis.[3] The incorporation of coordination groups is regarded as an efficient method to stabilize catalytic active species, and the ability is inevitably tied to the accessibility of versatile coordination ligands. Many monodentate and bidentate nitrogen-containing ligands were widely employed as functional groups of POFs,[4] but POFs containing terdentate units have not been reported so far.

[a] *State Key Laboratory of Structural Chemistry, Fujian Institute of Research on the Structure of Matter, Chinese Academy of Sciences, Fuzhou, Fujian 350002, China, E-mail: ruihu@fjirsm.ac.cn.*

[b] *Key Laboratory of Coal to Ethylene Glycol and Its Related Technology, Chinese Academy of Sciences, Fuzhou, Fujian 350002, China.*

Supporting information for this article is available on NMR data of the starting materials and hydrogenation products, Solid-state UV-vis spectra, TGA and XRD of BTP-POF and Pd/BTP-POF, N_2 and H_2 isotherms of BTP-POF and Pd/BTP-POF at 77 K under http://dx.doi.org/10.1002/cctc.200xxxxxx.

Pyridyl-centered heteroaromatic terdentate ligands, such as terpyridine, bis(oxazolinyl)pyridine and bis-(pyrazolyl)pyridine, have been extensively employed in the design and synthesis of supramolecular architectures and optoelectronic materials,[5,6] they may incorporate a variety of metal ions with favorable stability, some were used as supporting ligands of noble metals in catalytic reactions.[5] However, the synthesis of these terdentate ligands is cumbersome and labrious, it is even more difficult to introduce them into POFs as functional groups. Therefore, it is a great challenge to develop new strategies for facile synthesis of POFs containing pyridyl-centered terdentate units.

Click reaction between organic azides and terminal alkynes is well known to possess mild reaction conditions, wide group tolerance, superior modularity, high yield and regioselectivity.[7,8] The resultant 1,4-disubstituted 1,2,3-triazolyl can serve as a stable linkage for the connection of two chemical/biological components. Meanwhile, the importance of 1,2,3-triazolyl as a coordination group for the binding of metal ions and as a stabilizer of palladium nanoparticles (NPs) has been realized. Recently, several click-based POFs have been reported and their applications in gas storage and separation have been explored,[7b,9] but studies of click-based POFs in heterogeneous catalysis are seldom explored.

In our previous studies, we have prepared a series of ionic click-based nitrogen-containing ligands,[10] they can serve as efficient stabilizers of palladium NPs in catalysis. As a continuous effort to develop highly efficient and recyclable catalytic protocols,[11] we are interested in 2,6-bis(1,2,3-triazol-4-yl)pyridine (BTP), featuring two integral triazolyl moieties bridged by a central pyridyl core. BTP is readily available through simple click reaction and can serve as a terdenate linkage

of POFs. Inspired by its structural preference and strong chelating ability to metal ions, herein, we report a click-based POF containing chelating terdentate 2,6-bis(1,2,3-triazol-4-yl)pyridyl units, which can serve as an effective support for immobilization of palladium NPs with small size and narrow size distribution.

2. Experimental section

2.1 Materials and characterization

2,6-Diethynylpyridine[12] and tetrakis(4-azidophenyl)methane were prepared according to literature methods.[13] Other chemicals were commercially available and used without further purification. ^{1}H and ^{13}C NMR spectra were recorded on a Bruker AVANCE III NMR spectrometer at 400 and 100 MHz, respectively, using tetramethylsilane (TMS) as an internal standard and $CDCl_3$ as a locking solvent except where otherwise indicated. Solid-state ^{13}C CP/MAS NMR was performed on a Bruker SB Avance III 500 MHz spectrometer with a 4-mm double-resonance MAS probe, a sample spinning rate of 7.0 kHz, a contact time of 2 ms and pulse delay of 5 s. IR spectra were recorded with KBr pellets using Perkin-Elmer Instrument. Thermal gravimetric analysis (TGA) were carried out on NETZSCH STA 449C by heating samples from 30 to 800 ^{o}C in a dynamic nitrogen atmosphere with a heating rate of 10 °C·min^{-1}. Solid-state UV-vis spectra were recorded with $BaSO_4$ pellets on a Perkin-Elmer Lambda 35 UV-vis spectrophotometer. Powered X-ray diffraction (XRD) patterns were recorded in the range of 2θ = 5-85^{o} on a desktop X-ray diffractometer (RIGAKU-Miniflex II) with Cu Kα radiation (λ = 1.5406 Å). Nitrogen adsorption and desorption isotherms were measured at 77 K using a Micromeritics ASAP 2020 system. The samples were degassed at 100 ^{o}C for 5 h before the measurements. Surface areas were calculated from the adsorption data using Brunauer-Emmett-Teller (BET) and Langmuir methods. The pore size distribution curves were obtained from the adsorption branches using non-local density functional theory (NLDFT) method. Field-emission scanning electron microscopy (SEM) was performed on a JEOL JSM-7500F operated at an accelerating voltage of 3.0 kV. Transmission electron microscope (TEM) images were obtained with a JEOL JEM-2010 instrument operated at 200 kV. X-ray photoelectron spectroscopy (XPS) measurements were performed on a Thermo ESCALAB 250 spectrometer, using non-monochromatic Al Kα x-rays as the excitation source and choosing C 1s (284.6 eV) as the reference line. Elemental analyses were performed on an Elementar Vario MICRO Elemental analyzer. Inductively coupled plasma spectroscopy (ICP) was measured on Jobin Yvon Ultima 2. Gas chromatography (GC) was performed on a Shimadzu GC-2014 equipped with a capillary column (RTX-5, 30 m×0.25 μm) using a flame ionization detector.

Synthesis of BTP-POF

A mixture of 2,6-diethynylpyridine (0.255 g, 2.006 mmol), tetrakis(4-azidophenyl)methane (0.484 g, 0.999 mmol), $CuSO_4{\cdot}5H_2O$ (0.102 g, 0.408 mmol) and sodium ascorbate (0.162 g, 0.801 mmol) in dry DMF (30 mL) was stirred under nitrogen at 100 ^{o}C for 72 h to afford a dark yellow powder. The solid was isolated by filtration, and subsequently washed with aqueous EDTA-2Na solution (0.250 g in 200 mL H_2O), etnanol, and CH_2Cl_2 to remove any unreacted monomers or residues. The deep yellow powder was further treated by Soxhlet extraction in THF overnight and dried under reduced pressure at 80 ^{o}C for 12 h. Yield: 0.716 g (97 %). Elemental analysis calculated (%) of BTP-POF for $C_{43}H_{26}N_{14}$: C, 69.9; H, 3.5; N, 26.6. Found: C, 62.5; H, 4.8; N, 22.5. IR (KBr cm^{-1}): ν 3033 (w), 2952 (w), 1607 (w), 1575 (w), 1512 (s), 1451 (w), 1404 (w), 1234 (s), 1033 (s), 990 (s), 825 (s).

Synthesis of Pd/BTP-POF

BTP-POF (0.300 g) was added into a CH_2Cl_2 solution (300 mL) of palladium acetate (0.155 g, 0.689 mmol), the mixture was vigorously stirred at 60 ^{o}C for 24 h. The resulting product was washed thoroughly with CH_2Cl_2 to remove excess palladium acetate and dried under reduced pressure at 80 ^{o}C for 12 h. A 10-fold excess of aqueous $NaBH_4$ was added to stirring suspension of the above palladium polymer in water, the mixture was kept at room temperature for 3 h. The resultant black particles were collected by filtration, washed with water for several times, and dried in vacano at 80 ^{o}C for 12 h. Yield: 0.310 g (83 %). IR (KBr cm^{-1}): 3430 (s), 3148 (w), 3051 (w), 1609 (w), 1576 (w), 1514 (s), 1450 (w), 1397(w), 1233 (s), 1038 (s), 988 (s), 833 (s), 806 (s), 774 (w).

General procedures for hydrogenation of olefins

Hydrogenation was carried out in a high-pressure reactor equipped with a stirrer. A mixture of olefins (2 mL) and Pd/BTP-POF (0.0005 mol %) was stirred under 1.0 atm H_2 at 25 °C. After the reaction was completed, the product was removed from the reaction mixture with syringe, Conversion and selectivity were determined by GC, the identity of the products was confirmed by comparison with literature spectroscopic data.

General procedures for Recyclability tests

After hydrogenation reaction of 1-hexene in the presence of Pd/BTP-POF under 1.0 atm H_2 at 25 °C was finished, the product was removed directly from the reaction mixture with syringe, conversion and selectivity were determined by GC. The resultant catalytic species were dried in vacuo and reused for the next run with the recharge of 1-hexene.

3. Results and discussion

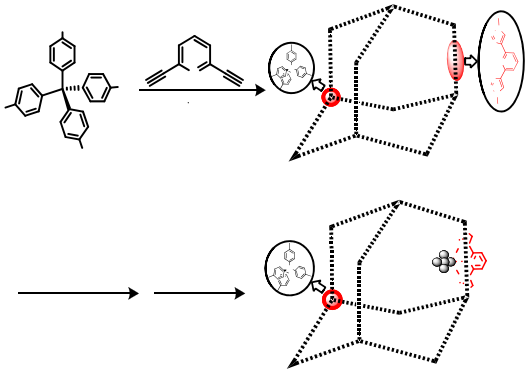

Scheme 1. Schematic illustration for synthesis of BTP-POF and Pd/BTP-POF.

As shown in Scheme 1, the reaction of 2,6-diethynylpyridine (DEP) and tetrakis(4-azidophenyl)methane (TAM) under the

standard click conditions gave rise to deep yellow BTP-POF in a 97% yield, subsequent treatment with $Pd(OAc)_2$ and reduction by $NaBH_4$ formed black Pd/BTP-POF in an 83 % yield. Both BTP-POF and Pd/BTP-POF are insoluble in water or common organic solvents. The Pd content in Pd/BTP-POF is 0.30 mmol g^{-1} as determined by ICP analysis. The structure and composition of BTP-POF were defined by IR, solid-state ^{13}C NMR and elemental analysis. IR spectra of starting materials and BTP-POF were shown in Figure 1. The strong peak at 3279 cm^{-1} and weak peak at 2100 cm^{-1} are ascribed to ≡C-H and C≡C stretching vibration of DEP, respectively. The characteristic peak of azido group in TAM was observed at 2121 cm^{-1}. The total disappearance of the three characteristic peaks in IR spectrum of BTP-POF suggests complete azide-alkyne cycloaddition. In comparison with TAM, the broader peak at 1607 cm^{-1} in BTP-POF may be ascribed to the overlap of N=N and C=C peaks, which further shows the formation of the expected 1,2,3-triazolyl linkage.[7b] The other peaks around 1575, 1512 and 1451 cm^{-1} are assigned to aromatic groups of the frameworks.[9]

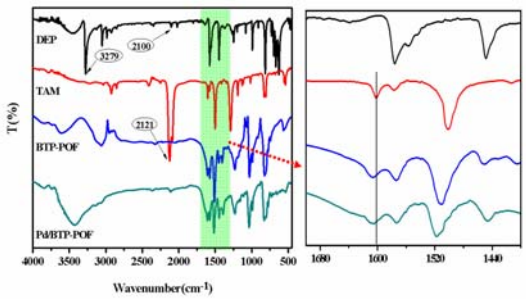

Figure 1. FTIR spectra of DEP, TAMB, BTP-POF and Pd/BTP-POF.

Solid-state ^{13}C NMR further confirms the formation of 1,2,3-triazolyl linkage. As shown in Figure 2, there is no characteristic peak of alkynyl in the range of 70-100 ppm, which demonstrates the efficiency of click reaction.[7b,14] The peak at 148 ppm corresponds to carbon atoms of pyridyl C=N and C_4-triazolyl. The signal at 135 ppm is assigned to the other carbon atom of 1,2,3-triazolyl ring and partial phenyl groups. The peak of the other phenyl carbon atoms was found at 120 ppm. The resonance at 64 ppm corresponds to central carbon atom of the tetraphenyl-methane core.[14,15] It should be mentioned that IR, solid-state UV-vis spectra (Fig. S1) and solid-state ^{13}C NMR spectra of Pd/BTP-POF are almost identical with that of BTP-POF, indicating structural preservation of BTP-POF after palladium loading. Two additional minor peaks at 179 and 22 ppm were observed in solid-state ^{13}C NMR spectrum of Pd/BTP-POF, which are assigned to carbonyl and methyl of the residual acetate, respectively.[4c]

Elemental analysis of BTP-POF shows that the experimental values of C and N are lower than respective theoretical values, the deviation mainly results from the presence of the trapped guest molecules, which is common in porous materials.[2,4] The presence of guest molecules was further supported by TGA (Fig. S2). The initial weight loss of 7.2 % in BTP-POF was observed before 100 °C. BTP-POF starts to decompose after 270 °C. The thermal stability of Pd/BTP-POF is lower than that of BTP-POF, which is probably ascribed to the presence of residual palladium acetate in the framework.[4c] XRD analysis indicates BTP-POF is amorphous (Fig. S3), which was ascribed to the kinetic-controlled irreversible process in click reaction.[16] The characteristic peak of palladium was also not observed in XRD spectrum of Pd/BTP-POF. SEM images show BTP-POF and Pd/BTP-POF are granular morphology with a size of 20-50 nm (Figure 3), palladium loading has no obvious effect on morphology of BTP-POF.

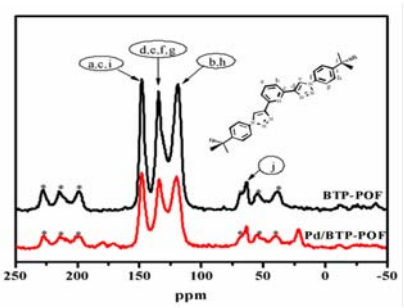

Figure 2. Solid-state ^{13}C NMR spectra of BTP-POF and Pd/ BTP-POF (* means interchangable assignment).

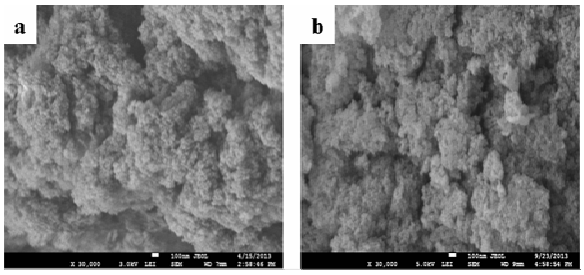

Figure 3. SEM images for BTP-POF (a) and Pd/BTP-POF (b)

The porosity and surface area of BTP-POF and Pd/BTP-POF were measured by nitrogen adsorption-desorption at 77 K. The nitrogen isotherm of BTP-POF exhibits a combination of type I and IV according to IUPAC classification, while Pd/BTP-POF gives an isotherm of type I (Fig. S4).[7b,17] The surface area of BTP-POF is 580 m^2 g^{-1}, which is decreased to 416 m^2 g^{-1} in Pd/BTP-POF owing to both partial pore filling and mass increment after palladium loading. The density of micropores decreases after palladium loading, but no significant change in size distribution of pores was observed (Fig. S3 inset). H_2 adsorption capacities of BTP-POF and Pd/BTP-POF at 77 K and 1 bar are 103 and 80 cm^3 g^{-1}, respectively (Fig. S5), which are comparable to those in MOFs, carbon materials and microporous polymers featuring similar or higher surface areas.[9c]

TEM analysis shows that palladium NPs were well dispersed in BTP-POF with a mean diameter of 1.8 nm and a standard deviation of 0.5 nm (Figure 4). It should be mentioned that the size of palladium NPs is smaller than those supported on POFs containing mono- or bi-dentate coordination groups,[2,4c] which is probably ascribed to strong coordination ability of terdentate BTP. Furthermore, a few of large NPs were also found at surface, which is probably ascribed to the dumpling to surface palladium species during the reduction.[15]

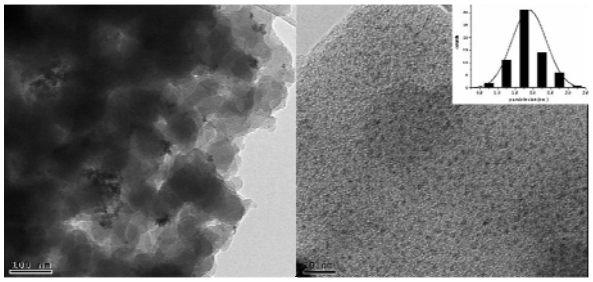

Figure 4. TEM images of Pd/BTP-POF.

The existing state of surface palladium in Pd/BTP-POF was investigated by XPS. As shown in Figure 5, Pd3d region was divided into two spin-orbital pairs, indicating the presence of two types of the surface-bound palladium species. The binding energy peaks at 335.9 (Pd $3d_{5/2}$) and 341.0 eV (Pd $3d_{3/2}$) are assigned to Pd(0) species, while the peaks at 337.5 (Pd $3d_{5/2}$) and 342.8 (Pd $3d_{3/2}$) correspond to Pd(II) species. A comparison of the relative areas of the integrated intensity of Pd(0) and Pd(II) shows the area ratio of Pd(0) to Pd(II) is 3/2. The presence of Pd(II) species is ascribed to the residual palladium acetate and/or reoxidation of Pd(0) during air contact.[4c,8] The $Pd3d_{5/2}$ binding energy at 335.9 eV for Pd(0) species in Pd/BTP-POF shifts positively by 0.5 eV in comparison with free Pd (335.4 eV).[5,18e] This positive shift may be ascribed to size effects and/or interaction of Pd(0) species with support, which makes Pd(0) species more electron-deficient than free Pd.[18d] On the other hand, the Pd $3d_{5/2}$ binding energy at 337.5 eV for Pd(II) species in Pd/BTP-POF shifts negatively by 0.9 eV in comparison with that of 338.4 eV for free $Pd(OAc)_2$,[4c] the negative shift further indicates the strong coordination of Pd(II) with chelating terdentate BTP units, in which the election donation from BTP to Pd(II) makes the Pd(II) species less electron-deficient.[4c]

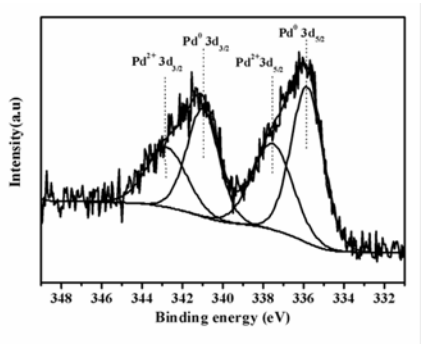

Figure 5. Pd3d XPS spectra of Pd/BTP-POF

In order to further confirm the interaction of supports and incorporated palladium species, XPS spectra of N1s of BTP-POF and Pd/BTP-POF were further investigated. As shown in Figure 6, N 1s region of BTP-POF was divided into two spin-orbital peaks with binding energy at 399.44 and 401.23 eV, and the area ratio of the two peaks is 2.6. However, the two spin-orbital peaks in Pd/BTP-POF shift to 399.57 and 401.35 eV, respectively, and the area ratio is increasded to 3.4. The shift of N 1s binding energy and the increment of the area ratio in Pd/BTP-POF further demonstrate strong interaction between BTP-POF and incorporated palladium species.

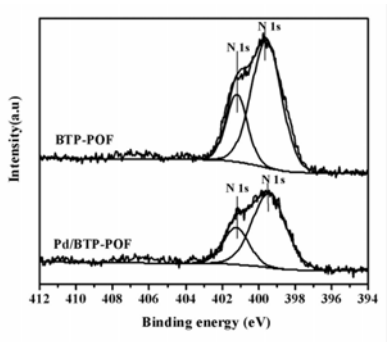

Figure 6. N1s XPS spectra of Pd/BTP-POF and BTP-POF

Table 1. Hydrogenation reactions of olefins[a].

Entry	Olefins	Time (h)	Con.[b] (%)	Sel.[b] (%)	TOF[c]
1	1-hexene	1	100	99	20000
2	1-hexene	2	100	100	10000
3[d]	1-hexene	2	0	0	0
4	1-octene	2	100	100	10000
5	cyclohexene	2	100	100	10000
6	1,3-cyclohexadiene	2	56	92	5600
7	1,3-cyclohexadiene	12	100	100	10000
8	styrene	2	100	100	10000
9	1-vinylimidazole	2	36	100	3600
10	1-hexene	5 min	22	31	-
11[e]	-	30 min	(22)	(32)	-

[a] Hydrogenation was performed in olefin (2mL) and Pd/BTP-POF [olefins (mol)/Pd (mol) = 20000] under 1.0 atm H_2; [b] Conversion and selectivity were determined by GC; [c] TOF based on mol product per mol palladium per hour; [d] BTP-POF was used in the absence of palladium; [e] filtration experiment.

Hydrogenation of olefins has been widely applied in pharmaceutical, agrochemical and petrochemical industries.[19] However, the use of POFs as heterogeneous supports in this reaction has seldom been reported. The catalytic performances of Pd/BTP-POF were investigated in hydrogenation reaction of 1-hexene under 1.0 atm H_2 at 25 °C. As shown in Table 1, when the reaction was performed with a olefin/[Pd] molar ratio of 20000 for 1 h, n-hexane was obtained in 100 % conversion and 99% selectivity (entry 1), TOF value of 20000 h^{-1} is higher than that from palladium NPs in nanoporous silica.[19f] Increasing reaction time to 2 h gave 100 % conversion and 100% selectivity (entry 2). As a comparison, the control experiment was performed in the presence of only BTP-POF, no hydrogenation product was

detected (entry 3). To extend scope of Pd/BTP-POF catalytic system, hydrogenation reactions of various olefins were examined. Both chain- and cyclo-alkene afford the corresponding products in a quantitative yield under the same conditions (entries 4 and 5). When the conjugate alkadiene 1,3-cyclohexadiene was used a substrate, a moderate conversion and 92% cyclohexane selectivity were obtained (entry 6), while a complete hydrogenation to cyclohexane can be achieved when reaction time was increased to 12 h. Interestingly, hydrogenation of styrene gave rise to the target product in a quantitative yield in 2 h (entry 8). The catalytic system is also efficient for hydrogeantion of 1-vinylimidazole, the target product was obtianed in 36 % conversion and 100% selectivity in 2h (entry 9).

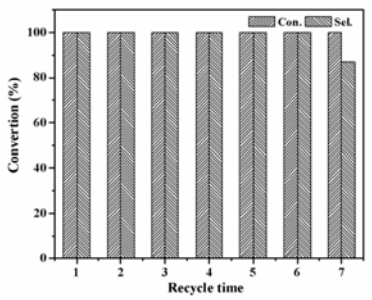

Figure 7. Recyclability of Pd/BTP-POF in hydrogenation of 1-hexene.

Besides high catalytic activity, stability and recyclability are also significant in a catalytic system. Recyclability of Pd/BTP-POF was evaluated in hydrogenation of 1-hexene under 1.0 atm H_2 at 25 ^oC for 2 h, After the reaction finishined and the product was separated, the residual catalytic species were used for next run with recharge of 1-hexene. Interestingly, 100 % conversion of 1-hexene and 100 % selectivity of n-hexane are maintained for 6 runs, and a slight decrement of selectivity was observed in the seventh run (Figure 7). The total TON (turnover number) exceeds 70,000. TEM analyses indicate that the mean diameter of palladium NPs is increased to 2.5 nm after recylcing for seven runs, but on obvious agglomeration was observed (Figure 8). Palladium leaching to organic phase, which was defined by ICP analysis, is 0.56 ppm after the first run. The outstanding stability and recycalibity of Pd/BTP-POF probably result from synergetic interaction of confinement of pores in BTP-POF and strong coordination of chelating terdentate nitrogen-containing groups with palladium, preventing palladium NPs from leaching and agglomeration during reaction and seprartion.

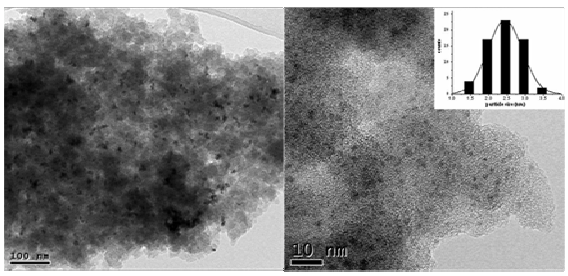

Figure 8. TEM images of Pd/BTP-POF after recycling seven runs.

Table 2 Summary of the poisoning experiments[a]

Entry	Additive	Ratio of the additive to palladium	Convertion	selectivity
1	Hg	-	100	97
2	CS_2	200	trace	-
3	PPh_3	200	60	62
4	pyridine	200	100	98
5	pyridine	2000	87	63

[a] The poisoning experiments were carry out with 1-hexene as a substrate in the presence of Pd/BTP-POF [olefins (mol) / Pd (mol) = 20000] under 1.0 atm H_2 at 25^oC for 2 h; [b] GC yield; [c] one drop of Hg was added.

To identify whether the catalytic system behaves in a heterogenous manner. Mercury drop test, poisoning and filtration experiments were carried out using 1-hexene as a substrate in the presence of Pd/BTP-POF. As shown in Table 2, when one drop of Hg(0) was added to reaction mixture before the reaction was initiated, there is no obvious effect on catalytic activity of Pd/BTP-POF (entry 1), which is mainly attributed to the repulsive interaction between Pd/BTP-POF and Hg(0), preventing the access of Hg(0) to palladium NPs. On the other hand, PPh_3, pyridine and CS_2 are commonly used as poisoning agents of palladium active speceis owing to their good binding ability to palladium.[20] When 200 equivalent amount of CS_2 was used as an additive in hydrogenation of 1-hexene, no catalytic activity was observed after 2h (entry 2). The addition of 200 equivalent amount of PPh_3 in the reaction mixture gives 60 % 1-hexene conversion and 62 % n-hexane selectivity (entry 3). However, the addition of 200 equivalent amount of pyridine results in 100 % conversion and 98% selectivity (entry 4), which are close to that under normal conditions (Table 1, entry 2). When pyridine loading was increased to 2000 equivalence, a serious poisoning with 87 % conversion and 63 % selectivity was observed (entry 5). The kinetic study further shows that the presence of pyridine results in lower catalytic activity and selectivity than that under normal conditions (Figure 9). The inhibiting effect is probably attributed to access of the additives to palladium NPs through cavities of BTP-POF. Noteworthily, after reaction was run for 5 min, the palladium-containing catalytic species was quickly removed by filtration, and the filtrate was continued for additional 25 min, negligible change in conversion and selectivity was observed (entries 10 and 11, Table 1), which indicates that hydrogenation proceeds in a heterogeneous pathway in the catalytic system.

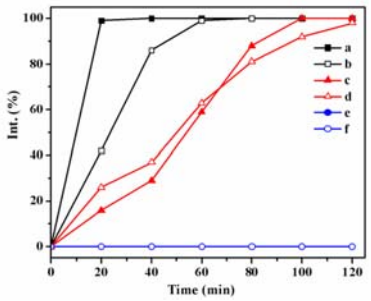

Figure 9. The conversion of 1-hexene and selectivity of hexane as a function of time in 1.0 atm H_2 at 25 °C: (a) conversion under normal conditions; (b) selectivity under normal conditions; (c) 1-hexene conversion after 200 equivalent amount of pyridine was added; (d) hexane selectivity after 200 equivalent amount of pyridine was added, (e) conversion after 200 equivalent amount of CS_2 was added.

Conclusions

A click-based POF containing chelating terdentate 2,6-bis(1,2,3-triazol-4-yl)pyridyl units has been presented. The POF can serve as an effective stabilizer of palladium nanoparticls (NPs) owing to synergetic interaction of confinement of pores and chelating coordination of the terdentate units. The well-dispersed palladium NPs with small size about 1.8 nm and narrow size distribution were readily obtained, they shows excellent catalytic activity, high stability and good reusability in palladium-catalyzed hydrogenation of olefins. the catalytic system behaves in a heterogeneous manner, no obvious loss of catalytic activity and agglomeration of palladium NPs were observed after recycling for seven runs. In summary, this study has demonstrated that click-based chelating terdentate units not only may act as the linakge of POFs, but also can serves as stabilizer of metal NPs in heterogerous catalysis, which provides a new strategy for facile construction of functional POFs containing chelating terdentate units.

Acknowledgements

This work was financially supported by 973 Program (2010CB933501, 2011CBA00502), Natural Science Foundation of China (21273239), Natural Science Foundation of Fujian Province (2011J01064) and “One Hundred Talent Project” from Chinese Academy of Sciences.

Reference

1. a) Y. Zhang and S. N. Riduan. *Chem. Soc. Rev.*, 2012, **41**, 2083-2094. b) X. Zou, H. Ren and G. Zhu. *Chem. Commun*., 2013, **49**, 3925-3936. c) S. Y. Ding and W. Wang. *Chem. Soc. Rev*., 2013, **42**, 548-568. d) P. Kaur, J. T. Hupp and S. T. Nguyen. *ACS Catal*., 2011, **1**, 819-835. e) N. B. McKeown and P. M. Budd. *Macromolecules*, 2010, **43**, 5163-5176.
2. a) C. E. Chan-Thaw, A. Villa, P. Katekomol, D. Su, A. Thomas and L. Prati. *Nano Lett*., 2010, **10**, 537-541. b) J. X. Jiang, C. Wang, A. Laybourn, T. Hasell, R. Clowes, Y. Z. Khimyak, J. l. Xiao, S. J. Higgins, D. J. Adams and A. I. Cooper. *Angew. Chem. Int. Ed*., 2011, **50**, 1072-1075. c) R. Palkovits, M. Antonietti, P. Kuhn, A. Thomas and F. Schüth. *Angew. Chem. Int. Ed.*, 2009, **48**, 6909-6912. d) Z. Xie, C. Wang, K. E. deKrafft and W. Lin. *J. Am. Chem. Soc.*, 2011, **133**, 2056-2059..
3. a) Q. Zhang, S. Zhang and S. Li. *Macromolecules*, 2012, **45**, 2981-2988. b) H. Urakami, K. Zhang and F. Vilela. *Chem. Commun*., 2013, **49**, 2353-2355. c) A. M. Shultz, O. K. Farha, J. T. Hupp and S. T. Nguyen. *Chem. Sci*., 2011, **2**, 686-689. d) P. Zhang, Z. Weng, J. Guo and C. Wang. *Chem. Mater*., 2011, **23**, 5243-5249. e) F. Vilela, K. Zhang and M. Antonietti. *Energy Environ. Sci.*, 2012, **5**, 7819-7832.
4. a) Y. Jin, Y. Zhu and W. Zhang. *CrystEngComm*, 2013, **15**, 1484-1499. b) N. Kang, J. H. Park, K. C. Ko, J. Chun, E. Kim, H. W. Shin, S. M. Lee, H. J. Kim, T. K. Ahn, J. Y. Lee and S. U. Son. *Angew. Chem. Int. Ed*., 2013, **52**, 1-6. c) S. Y. Ding, J. Gao, Q. Wang, Y. Zhang, W. G. Song, C. Y. Su and W. Wang. *J. Am. Chem. Soc*., 2011, **133**, 19816-19822.
5. a) M. Ostermeier, M. A. Berlin, R. M. Meudtner, S. Demeshko, F. Meyer, C. Limberg and S. Hecht. *Chem. Eur. J*., 2010, **16**, 10202-10213. b) R. M. Meudtner, M. Ostermeier, R. Goddard, C. Limberg and S. Hecht. *Chem. Eur. J*., 2007, **13**, 9834-9840. c) Y. Li, J. C. Huffman and A. H. Flood. *Chem.Commun*., 2007, 2692-2694. d) T. R. Chan, R. Hilgraf, K. B. Sharpless and V. V. Fokin. *Org. Lett.*, 2004, **6**, 2853-2855. e) J. D. Crowley and P. H. Bandeen. *Dalton Trans*., 2010, **39**, 612-623.
6. a) G. Desimoni, G. Faita and P. Quadrelli. *Chem. Rev.*, 2003, **103**, 3119-3154. b) M. A. Halcrow and Coord. *Chem. Rev.*, 2005, **249**, 2880-2908. c) V. Balzani, A. Juris, M. Venturi, S. Campagna and S. Serroni. *Chem. Rev.*, 1996, **96**, 759-833. d) O. Sato, J. Tao and Y. Z. Zhang. *Angew. Chem. Int. Ed.*, 2007, **46**, 2152-2187.
7. a) P. Kuhn, M. Antonietti and A. Thomas. *Angew. Chem. Int. Ed*., 2008, **47**, 3450-3453. b) P. Pandey, O. K. Farha, A. M. Spokoyny, C. A. Mirkin, M. G. Kanatzidis, J. T. Hupp and S. T. Nguyen. *J. Mater. Chem.*, 2011, **21**, 1700-1703.
8. C. Barner-Kowollik, F. E. D. Prez, P. Espeel, C. J. Hawker, T. Junkers, H. Schlaad and W. V. Camp. *Angew. Chem. Int. Ed*., 2011, **50**, 60-62.
9. a) D. J. V. C. Steenis, O. R. P. David, G. P. F. Strijdonck, J. H. Maarseveen and J. N. H. Reek. *Chem.Commun*., 2005, 4333-4335. b) C. R. Becer, R. Hoogenboom and U. S. Schubert. *Angew. Chem. Int. Ed*., 2009, **48**, 4900-4908. c) O. Plietzsch, C. I. Schilling, T. Grab, S. L. Grage, A. S. Ulrich, A. Comotti, P. Sozzani, T. Muller and S. Bräse. *New J. Chem*., 2011, **35**, 1577-1581.
10. a) D. Zhang, C. S. Zhou and R. H. Wang. *Catal. Commun.*, 2012, **22**, 83-88. b) F. Z. Kong, C. S. Zhou, J. Y. Wang, Z. Y. Yu and R. H. Wang. *ChemPlusChem*, 2013, **78**, 536-545. c) L. Y. Li, J. Y. Wang, T. Wu and R. H. Wang. *Chem. Eur. J.,* 2012, **18**, 7842-7851.
11. a) H. X. Zhao, X. X. Li, J. Y. Wang, L. Y. Li and R. H. Wang. *ChemPlusChem*, 2013, **78**, 1491-1502. b) L. Y. Li, Z. L. Chen, H. Zhong and R. H Wang. *Chem Eur J.*, 2014, **20**, 3050-3060. c) C. S. Zhou, J. Y. Wang, L. Y. Li, R. H. Wang and M. C. Hong, *Green Chem.*, 2011, **13**, 2100-2106
12. S. Leininger, M. Schmitz and P. J. Stang. *Org. Lett*., 1999, **1**, 1921-1923.
13. O. Plietzsch, C. I. Schilling, M. Tolev, M. Nieger, C. Richert, T. Muller and S. Bräse. *Org. Biomol. Chem*., 2009, **7**, 4734-4743.
14. W. Lu, D. Yuan, D. Zhao, C. I. Schilling, O. Plietzsch, T. Muller, S. Bräse, J. Guenther, J. Blümel, R. Krishna, Z. Li and H. C. Zhou. *Chem. Mater*., 2010, **22**, 5964-5972.
15. a) J. M. Jin, J. M. Lee, M. H. Ha, K. Lee and S. Choe. *Polymer*, 2007, **48**, 3107-3115. b) J. X. Jiang, F. Su, H. Niu, C. D. Wood, N. L. Campbell, Y. Z. Khimyak and A. I. Cooper. *Chem. Commun*., 2008, 486-488.
16. a) T. Muller and S. Bräse. *Angew. Chem. Int. Ed*., 2011, **50**, 11844-11845. b) K. S. W. Sing, D. H. Everett, R. A. W. Haul, L. Moscou, R. A. Pierotti, J. Rouquerol and T. Siemieniewska. *Pure Appl. Chem*., 1985, **57**, 603-619.
17. T. Hasell, C. D. Wood, R. Clowes, J. T. A. Jones, Y. Z. Khimyak, D. J. Adams and A. I. Cooper. *Chem. Mater*., 2010, **22**, 557-564.
18. a) A. F. Lee, S. F. J. Hackett, J. S. J. Hargreaves and K. Wilson. *Green Chem.*, 2006, **8**, 549-555.41. b) V. Z. Radkevich, T. L. Senko, K. Wilson, L. M. Grishenko, A. N. Zaderko and V. Y. Diyuk. *Appl. Catal. A: Gen.*, 2008, **335**, 241-251. c) Z. Bastl. *Collect. Czech. Chem. Commun.* 1995, **60**, 383-392. d) W. J. Gammon, O. Kraft, A. C. Reilly and B. C. Holloway. *Carbon*, 2003, **41**, 1917-1923.
19. a) L. M. Baldyga, S. O. Blavo, C. H. Kuo, C. K. Tsung and J. N. Kuhn. *ACS Catal*., 2012, **2**, 2626-2629. b) N. Linares, S. Hartmann,

A. Galarneau and P. Barbaro. *ACS Catal*., 2012, **2**, 2194-2198. c) Y. Jiang, J. Hess, T. Fox and H. Berke. *J. Am. Chem. Soc.*, 2010, **132**, 18233-18247. e) A. V. Biradar, A. A. Biradar and T. Asefa. *Langmuir*, 2011, **27**, 14408-14418. f) Y. Wang, A. V. Biradar, C. T. Duncan and T. Asefa. *J. Mater. Chem.*, 2010, **20**, 7834-7841. g) Y. Zhu, Y. Kang, Z. Zou, Q. Zhou, J. Zheng, B. Xia and H. Yang. *Fuel Cells Bulletin*, 2008, 12-15. h) O. M. Wilson, M. R. Knecht, J. C. G. Martinez and R. M. Crooks. *J. Am. Chem. Soc.*, 2006, **128**, 4510-4511

20. a) H. Zhong, J. Y. Wang, L. Y. Li and R. H. Wang, *Dalton Trans*, 2014, **43**, 2098-2103. b) K. O. Sebakhy, S. Kessel and M. J. Monteiro. *Macromolecules*, 2010, **43**, 9598-9600. c) S. Okada, K. Mori, T. Kamegawa, M. Che and H. Yamashita. *Chem. Eur. J*., 2011, **17**, 9047-9051. d) M. Graeser, E. Pippel, A. Greiner and J. H. Wendorff. *Macromolecules*, 2007, **40**, 6032-6039. e) M. J. Monteiro. *Macromolecules*, 2010, **43**, 1159-1168.